Caenorhabditis elegans neuronal regeneration is influenced by life stage, ephrin signaling, and synaptic branching

Zilu Wu*†‡, Anindya Ghosh-Roy*, Mehmet Fatih Yanik§, Jin Z. Zhang¶, Yishi Jin*†‡, and Andrew D. Chisholm*†‖

*Division of Biological Sciences, Center for Molecular Genetics, and ‡Howard Hughes Medical Institute, University of California at San Diego, La Jolla, CA 92093; †Department of Molecular, Cell, and Developmental Biology, Sinsheimer Laboratories, University of California, Santa Cruz, CA 95064; §Department of Physics, Stanford University, Palo Alto, CA 94305; and ¶Department of Chemistry and Biochemistry, University of California, Santa Cruz, CA 95064

Communicated by Cornelia I. Bargmann, The Rockefeller University, New York, NY, July 26, 2007 (received for review May 15, 2007)

We previously reported functional regeneration of *Caenorhabditis elegans* motor neurons after femtosecond laser axotomy. We report here that multiple neuronal types can regrow after laser axotomy using a variety of lasers. The precise pattern of regrowth varies with cell type, stage of animal, and position of axotomy. Mechanosensory axons cut in late larval or adult stages displayed extensive regrowth, yet failed to reach their target area because of guidance errors in the anteroposterior axis. By contrast, mechanosensory axons cut in early larval stages regrew at the same rate but with fewer anteroposterior guidance errors, and were more likely to reach their target area. In adult animals lacking the VAB-1 Eph receptor tyrosine kinase, mechanosensory axon regrowth was more accurate than in the wild type, suggesting that guidance errors of regrowing touch neuron axons are the result of Eph signaling. Kinase-dependent and kinase-independent Eph signaling influenced outgrowth and guidance of regrowing touch neurons, respectively. Mechanosensory neurons regrew when severed proximal to their collateral synaptic branch but did not regrow when severed distal to the branch point. However, the distal axon could regrow if the branch is removed surgically at the same time as distal axotomy, or at a later time. The touch neuron synaptic branch point may act as a sorting area to regulate growth. These findings reveal that multiple influences affect regenerative growth in *C. elegans* neurons.

axotomy | laser | femtosecond laser | microsurgery

Regeneration of neuronal processes after injury has been studied at the cellular level since the days of Ramon y Cajal (1). Axons of most vertebrates and invertebrates display strong regenerative responses. Axons that successfully regenerate can form a new growth cone at the cut tip of the axon within hours of damage. Formation of a new growth cone after injury involves elevation of intracellular calcium (2), several intracellular signaling pathways (3), and local protein synthesis (4). Axotomy-induced signals may feed into growth cone initiating pathways related to those used in developmental collateral branching. The regenerated growth cone then undergoes a transition from sprouting to elongation growth mode; regenerating and developmental axon growth may involve both common and distinct molecular pathways (5).

Central neurons in mammals and birds fail to regenerate after axotomy, partly because of the inhibitory environment of the CNS (6). Intensive analysis has identified several inhibitory components of myelin (7), as well as of the astrocytic glial scar (8). The inhibitory components of mammalian myelin interact with a neuronal receptor complex (9, 10) that represses axon growth via the small GTPase Rho (11). Inhibitory influences of the CNS environment are not absolute, and can be overcome by various treatments, such as conditioning peripheral lesions that increase the intrinsic ability of CNS axons to regrow (12).

We are interested in the fundamental conserved aspects of neuronal regeneration. Until recently, there has been little analysis of axon regeneration in genetically tractable model organisms. Although myelinated, Zebrafish CNS axons display spontaneous regeneration (13), studies of which have revealed the importance of cAMP in promoting regrowth *in vivo* (14). Needles have been used to generate large-scale brain injuries to study the responses of *Drosophila* central neurons to damage (15), and surgical removal of sense organs has been used to analyze degenerative processes in sensory neurons (16).

We previously used an amplified femtosecond laser to cut identified GFP-labeled axons in *Caenorhabditis elegans* and found that motor neurons can regrow and restore function (17). Femtosecond laser surgery has also been used to cut the sensory dendrites of *C. elegans* chemosensory neurons although these were found not to regenerate (18). Here, we report that multiple neuron types in *C. elegans* regrow in response to axotomy, using a variety of laser types. However, *C. elegans* neurons are not fully competent for regeneration. We report that regrowth responses are strongly influenced by larval stage. Eph signaling influences the accuracy of regeneration in adult mechanosensory neurons. Finally, we show that the synaptic branch point of mechanosensory neurons defines a transition point in the regrowth potential of an axon.

Results

Cutting *C. elegans* Axons Using Femtosecond and Conventional Lasers. We previously reported cutting individual neuronal processes in *C. elegans* using an amplified femtosecond laser (17). We have since found that axons can be cut using a high repetition rate unamplified femtosecond laser (80–90 MHz) mode or a conventional UV laser of the type used for *C. elegans* cell ablations (19). There are several differences in the immediate responses of axons cut with the different lasers [supporting information (SI) Table 1 and SI Fig. 5]. High repetition rate ("MHz") femtosecond laser axotomy creates a gap of 2–5 μm within seconds of cutting, whereas low repetition rate ("kHz") laser axotomy is more precise, creating smaller gaps (1–2 μm; see SI Movie 1). These gaps expand over several hours because of retraction of both cut ends. Unamplified MHz or UV lasers often create damage to the surrounding epidermis visible as autofluorescent

Author contributions: Y.J. and A.D.C. designed research; Z.W. and A.G.-R. performed research; Z.W., A.G.-R., M.F.Y., and J.Z.Z. contributed new reagents/analytic tools; Z.W., A.G.-R., and A.D.C. analyzed data; and Y.J. and A.D.C. wrote the paper.

The authors declare no conflict of interest.

Freely available online through the PNAS open access option.

Abbreviations: AP, anteroposterior; CD, cavity dumped; FWHM, full width half maximum.

‖To whom correspondence should be addressed. E-mail: chisholm@ucsd.edu.

This article contains supporting information online at www.pnas.org/cgi/content/full/0707001104/DC1.

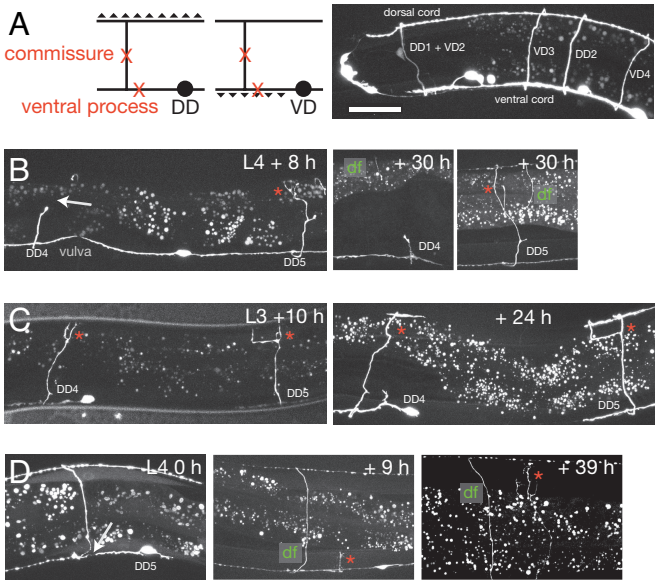

Fig. 1. Regrowth of D motor neurons after axotomy. (*A*) D neuron morphology and synaptic polarity; triangles indicate neuromuscular junctions; X marks indicate sites of axotomy in mid lateral commissure and in ventral cord. Confocal of D neuron morphology in L4 stage, *juIs76* marker. (Scale bar: 20 μm.) (*B*) When D neuron commissures were cut at the mid lateral position (arrow), they retracted as far as the lateral edges of the muscle quadrants. Proximal stumps of cut D commissures became swollen and began to sprout within 6–12 h of cutting. Most DD neurons cut in the L4 stage regrew to the dorsal cord within 8–10 h (e.g., 21/23 DD5s). In all figures, red asterisks indicate a regrown process, and df denotes the distal fragment of the cut axon. Midbody D neurons become unable to regrow dorsally as the reproductive system develops. Neurons DD4 + DD5 (marker *juIs145*) were cut in L4 stage. At 30 h, DD4 has not grown, whereas DD5 has reached the dorsal cord. (*C*) DD4 and DD5 (marker *ynIs37*) cut in L3 stage; both regrow to dorsal cord by 10 h. Note splitting and lateral extension of both regrowing processes as they meet dorsal muscle (*), similar to the behavior of VD growth cones in development (31); one of the DD4 branches has been pruned by 24 h. (*D*) Growth of new DD5 commissure to dorsal cord after cutting in ventral process (arrow, 0 h), L4 stage *juIs145*.

scars (SI Fig. 5 *A* and *F*), around which the regrowing axon often extends (e.g., Fig. 3*A*). After kHz axotomy no scarring is seen; axons cut in this way occasionally (<10%) repair themselves by fusion with the distal fragment within 6 h of cutting. By using kHz lasers, axons can be cut with only 10 pulses of 20 nJ each. Axons cut using any of the three laser types regrow after a lag period of 6–24 h depending on the cell type; the rate of regrowth and the total distance grown after injury were not significantly different between axons cut with the different lasers (SI Fig. 5*E*). In the analyses presented here we chose to use femtosecond lasers in the MHz mode.

Motor Neurons and Chemosensory Neurons Can Regrow After Axotomy. In our earlier studies, we reported that GABAergic D type motor neurons (Fig. 1*A*) showed robust regeneration when severed in the L4 stage using an amplified femtosecond laser (17). We confirmed that ≈70% of DD and VD commissures cut in the L4 stage regrew after axotomy using the MHz femtosecond laser (Fig. 1*B*; $n = 49$). Axotomized D neuron commissures formed swollen tips or growth cones by 8–12 h and thereafter extended dorsally at rates of 2–3 μm/h. We found no consistent differences in the ability of DD and VD neurons to regrow, with the exception of the midbody neurons DD4 and VD8. DD4 and VD8 either did not extend sprouts or grew laterally and ventrally after cutting; regrowing DD4 or VD8 cells rarely reached the dorsal midline (2/23 DD4 and 1/9 VD8 reached the dorsal cord at 24 h; Fig. 1*B*). Two cells that develop in the midbody of the L4 hermaphrodite, the uterine seam cell and the vul E cell, are connected to the lateral epidermis (20) and might physically block the regrowth of nearby commissures.

To test whether the development of these structures might account for the inability of DD4/VD8 to regrow, we cut DD cells in the L2 or L3 stages and found that all DD cells, including DD4, could regrow to the dorsal midline (5/6 DD4s regrew by 10 h; Fig. 1*C*). The failure of midbody motor commissures to regenerate in the L4 stage is likely a result of the development of the reproductive structures.

In these experiments, commissures were cut in mid lateral positions, 20–30 μm from their target areas in the dorsal cord. To test whether motor neurons could regenerate when cut further from their target area we severed DD axons within the ventral nerve cord of L4 animals, between the cell body and the commissural branch (Fig. 1*A*). Three of six DD5s extended new commissures to the dorsal midline (Fig. 1*D*), showing that DD neurons can regrow an entire commissure after injury.

To explore the generality of these findings we next tested the regenerative responses of chemosensory neurons, which are bipolar neurons with ciliated sensory dendrites. Sensory dendrites of dye-filled phasmid neurons do not regrow when cut with amplified lasers (17, 18). Using unamplified MHz laser cutting of GFP-marked neurons we confirmed that phasmid processes did not regrow when cut (SI Fig. 6*B*). The dendrites of the ciliated sensory neurons ADF and ASH do not regrow after amplified femtosecond laser surgery (18). We tested whether these findings extended to a chemosensory neuron with a complex cilium, AWB. AWB dendritic processes severed in the L4 stage frequently regrew (5/11 AWB cells showed sprouting), although more slowly than motor or mechanosensory neurons (SI Fig. 6 *D* and *E*). Regrowing AWB processes extended anteriorly and in one case regrew to the tip of the nose. These observations show that some chemosensory dendrites can regrow after injury.

Accuracy of Mechanosensory Neuron Process Regrowth Declines with Age. We previously showed that mechanosensory axons can regrow when cut using amplified femtosecond lasers (21). We confirmed and extended these observations using MHz axotomy. Mechanosensory neurons are bipolar, with long anterior sensory axons and short posterior axons; their synaptic output is from collateral branches formed from their anterior axons (Fig. 2*A*). We first cut ALM axons at ~30% of their length (30–50 μm from the ALM cell body); we cut PLMs at similar distances from their cell bodies. The sequence of changes after axotomy in touch neurons paralleled that observed in motor neurons: after several hours the proximal stump swelled and developed a growth cone with filopodial protrusions between 10 and 24 h. Between 24 and 48 h ALM axons extended at 7.0 ± 0.9 μm/h (Fig. 2*B*). Most (38/48) ALMs cut in the L4 or in young adults sprouted and regrew from the proximal stump; in only two cases the axon regrew from a new collateral branch. Newly formed axons initially grew anteriorly but randomly strayed dorsally or ventrally; many reversed direction and extended posteriorly (11/18 L4s/young adults; Fig. 2*B*), and some of these reversed again to form loops (*cf.* PLM, Fig. 3*A*). In some cases the axotomized axon did not regrow; instead, the uninjured posterior axon grew out (4/18 L4 ALMs; SI Fig. 7). Regrowing touch neurons frequently extended additional branches by 24 h, most of which were pruned by 48 h. For example, 19 PLMs cut in the L4 stage extended 31 collateral branches at 24 h, 17 of which had disappeared by 48 h (we define a branch as an extension >2 μm). Nevertheless, although ALM axons regrew 159 ± 23 μm in 48 h after axotomy, they failed to reach their targets in the nerve ring when cut in L4 or young adult (0/13 L4s; 0/32 young adults).

The response of mechanosensory neurons to axotomy in early

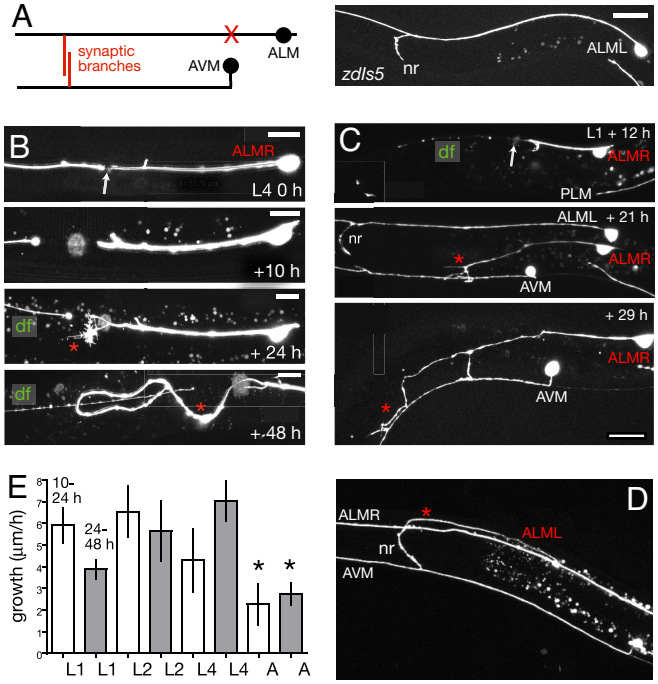

Fig. 2. Decline in guidance of touch neuron regrowth during larval development. (*A*) Anatomy of anterior touch neurons ALM and AVM. X, site of axotomy in ALM, proximal to the synaptic branch in the nerve ring (nr). (*B*) Aberrant regrowth of ALML after axotomy in mid L4 stage. A growth cone is visible at 24 h; by 48 h, the regrown process has reversed posteriorly; the distal fragment (df) is beaded yet clearly visible at 48 h. (*C*) Regrowth of ALML after axotomy in L1 stage. At 12 h, the proximal stump of ALMR has formed a growth cone but has not yet begun to extend; the distal fragment is faint and beaded. By 21 h, ALMR has extended anteriorly and ventrally, sending two branches to the ventral cord (marked by AVM process); the ALMR distal fragment is no longer visible. By 29 h, ALMR has reached the nerve ring; one of the ventral cord branches has retracted. (Scale bars: 10 μm.) (*D*) ALML regrowth into the nerve ring (nr) 24 h after axotomy in L1. The regenerated ALM (*) lacks the anterior process distal to the synaptic branch. (*E*) Growth rates of ALM between 10 and 24 h and 24 and 48 h (gray bars) after axotomy in different stages; mean ± SEM; $n > 5$ for each; only adult growth rates are significantly slower (*t* test). *, $P < 0.05$.

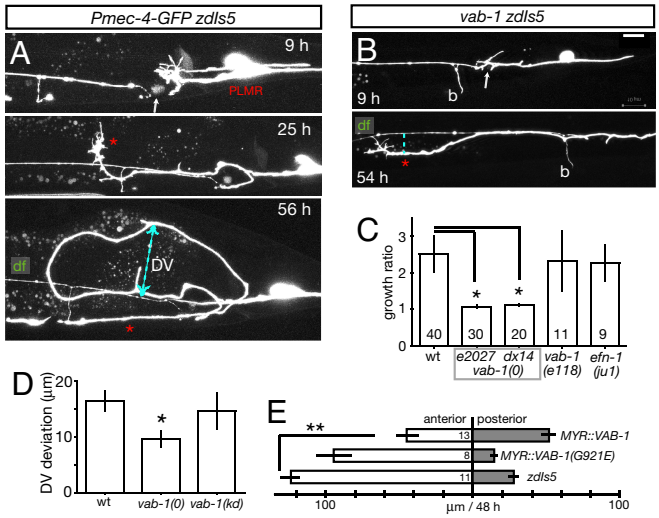

Fig. 3. Eph signaling influences guidance of regrowing touch neurons. (*A*) PLM processes cut in L4 stage proximal to the branch point by using MHz laser, marker *zdIs5*. Note prominent growth cones at 9–25 h and posterior turning between 25 and 56 h. (*B*) PLM axons turn less in *vab-1*(*e2027*) background; b, PLM branch. (Scale bar: 10 μm.) (*C*) Growth ratio (total distance grown by axon divided by net distance from cut site to tip of axon) in wild type, *vab-1* null and kinase-dead (*e118*) mutants, and *efn-1*(*ju1*). The total regrowth of PLMs at 24 h was not significantly different (wt, 100 ± 18 μm; *vab-1*, 64 ± 8 μm; $P = 0.09$ by *t* test). (*D*) maximum dorsoventral distance (DV, dashed line in 56 h panel) of regrown processes from distal fragment, in wild type, *vab-1*(*e2027*), *vab-1*(*e118*) animals cut as L4s and scored 48 h later. (*E*) Regrowth of anterior and posterior processes after anterior axotomy in MYR::VAB-1 (*quIs5*) and MYR::VAB-1(G912E) (*quIs4*) L4 animals, and WT controls; all strains contain the *zdIs5* marker. Anterior regrowth is significantly reduced only in *quIs5* expressing animals. *, $P < 0.05$; **, $P < 0.01$.

larval stages was dramatically different from that in later stages. After axotomy in the L1 stage, 50% (8/16) of ALM axons regrew to the nerve ring within 24 h. Regrowing axons did not simply fuse with distal fragments as most took different routes to the nerve ring, and failed to regrow the anterior extension to the nose (Fig. 2*C*). Both the duration of the quiescent period and rate of growth after axotomy in the L1 were comparable with that after axotomy in the L4 (Fig. 2*E*). ALM neurons cut in the L2 stage also regrew to the nerve ring, although slightly less frequently (3/11). Overall, ALM axons cut in the L1/L2 stages were less likely to reverse in the anteroposterior (AP) axis or extend posterior processes than when they were cut in L4 or young adult (3/22 L1/L2 vs. 11/18 L4/adult, $P < 0.01$ by Fisher exact test). Touch neurons cut in early larval stages were less likely to extend additional branches than those cut in later stages (3/16 touch neuron axons extended side branches 24 h after L1 axotomy, versus 19/37 in L4 stage; $P < 0.05$).

After its primary outgrowth in the embryo, the ALM axon grows proportionally during larval development (22). The ALM axon, measured from cell body to synaptic branch, grows from 74.2 ± 4 μm in the L1 to 217 ± 7 μm in L4, and to 303 ± 13 μm in 1-day old adults ($n = 7$). The reduced ability of later larval axons to reach their targets could in part reflect decreased proportional growth as opposed to growth-cone dependent outgrowth. However, the total increase in process length after axotomy was not significantly different in L4 versus L1 animals (159 ± 23.8 μm in L4 vs. 178 ± 16.4 μm in L1, between 0 and 48 h; $n = 7$). Only adults showed a decreased growth rate relative to L1s (Fig. 2*E*). Finally, after axotomy in the L1 and L2 stages the distal fragments became thin, beaded and often invisible within 24 h (Fig. 2*C*). By contrast, after axotomy in L4s or young adults, the distal fragment became fainter and had a beaded morphology, yet remained visible for several days, suggesting that the rate of removal or degeneration of the distal fragment also decreases with larval stage. We conclude that the primary reason regrowing mechanosensory neurons fail to reach their targets in later larval stages is their aberrant guidance, although decreases in axon growth and the persistence of distal fragments may also play a role.

Eph Receptor Signaling Affects Guidance of Regrowing PLM Processes. The aberrant guidance of touch neurons in later larval stages could be due to loss of their normal guidance cues, or it might reflect inappropriate or elevated responsiveness to other cues. Ephrins are conserved axon guidance cues in vertebrates and in *C. elegans* (23), and ephrin signaling influences regenerative axon growth in vertebrates (24). In *C. elegans* mutants lacking the VAB-1 Eph receptor the PLM axon sometimes overshoots (25). We therefore tested whether ephrin signaling might contribute to guidance errors in regrowth of the touch neurons. The rate of PLM regrowth was not significantly different in *vab-1* null mutants compared with wild type (mean rates 3.1 ± 0.5 μm/h in *zdIs5* ($n = 12$), 2.1 ± 0.4 μm/h in *vab-1 zdIs5* ($n = 18$); $P = 0.15$). However PLM regrowth in *vab-1* mutants was straighter than in the wild type: in *vab-1* mutants axotomized PLM axons rarely reversed direction in the AP axis and remained closer to their original trajectory (Fig. 3*B*). To quantify these effects on guid-

ance we calculated the ratio of the total distance extended by the axon divided by the net distance, measured as a straight line from the site of axotomy to the tip of the axon. In the wild type the regrowing axon extended on average 2.9 times its net distance whereas *vab-1* axons extended 1.1 times their net length ($P = 0.04$, unpaired t test; Fig. 3*C*). These results suggest impaired guidance of PLM regrowth in adults is due to Eph signaling. Eph receptors are bidirectional signaling molecules that can stimulate "forward" kinase-dependent signaling into the Eph receptor-expressing cell, or reverse signaling into ephrin-expressing cells (26). To test whether the misguidance of regrowing axons required forward or reverse Eph signaling we cut PLM in animals lacking VAB-1 kinase activity [*vab-1(e118)*] and observed wild-type like deviation (Fig. 3 *C* and *D*). This result suggests that the abnormal guidance of PLMs may involve kinase-independent functions of VAB-1 Eph receptor. Axotomy of animals lacking the EFN-1 ephrin also resulted in wild type-like misguidance (Fig. 3*C*). As ephrins have redundant roles in developmental PLM outgrowth (25), they may also be redundant in regrowth.

Expression of a myristoylated VAB-1 intracellular domain (MYR::VAB-1) in touch neurons causes premature termination of PLM axon outgrowth because of constitutive activation of the VAB-1 kinase-dependent "forward signaling" pathway (25). We tested whether VAB-1 forward signaling might also influence PLM regrowth, as opposed to guidance. Axotomized PLM axons expressing MYR::VAB-1 (*quIs5*) displayed significantly less anterior regrowth than the wild type (45.52 ± 14.5 μm *quIs5* vs. 125.0 ± 13.4 μm WT outgrowth in 48 h, $P < 0.01$ by ANOVA) or animals expressing a control kinase-dead MYR::VAB-1(G912E) (*quIs4*; Fig. 3*E*). Instead, MYR::VAB-1 expressing PLM neurons frequently extended their uninjured posterior axons (Fig. 3*E*). We infer that activation of VAB-1 forward signaling does not globally inhibit regrowth but may elevate sensitivity of the anterior axon to repellent cues, triggering growth of the uninjured axon. Taken together, VAB-1 signaling seems to play two distinct roles in PLM regrowth: a kinase-independent role in guidance, and a kinase-dependent role that represses anterior growth.

The Synaptic Branch of Touch Neurons Marks a Transition in Regenerative Capacity. The synaptic output of mechanosensory neurons is confined to their collateral branches to the nerve ring (ALM) or to the ventral cord (PLM). Studies on *C. elegans* synapse-defective mutants have suggested that formation of stable synaptic branches may repress axon growth (27). We therefore tested how the synaptic branch influences regrowth after axotomy. We first cut PLM axons immediately proximal or distal to their synaptic branch in the L4 stage. When we cut PLM 10 μm proximal to the branch, it consistently regrew as described above (Figs. 3*A* and 4*E*). By contrast, when we cut the PLM axon 10 μm distal to its branch, almost no regrowth occurred up to 48 h post cutting (Fig. 4*A*, 3/25, *zdIs5*; 0/11, *muIs32*). The PLM synaptic branch also did not regrow when cut (Fig. 4*B*; 0/8 *zdIs5*, 0/7 *muIs32*); instead, the stump of the branch retracted to the axon such that the branch could not be found after 24 h. Cutting the axon distal to the branch occasionally resulted in a small amount of growth of the branch (Fig. 4 *A* and *E*); however, cutting the branch alone had no significant effect on growth of the distal axon (data not shown). The inhibitory effect of the synaptic branch is not unique to PLM, as we observed a similar effect of the ALM synaptic branch (SI Fig. 8 *B–D*).

In the course of these experiments we observed that the position of the PLM branch varied depending on the transgenic background used. In *muIs32* animals the PLM branch is in its correct position, just posterior to the vulva, whereas in *zdIs5* the PLM branch is more posterior. Axons cut proximal to the branch in *muIs32* animals regrew, even though they were further from the cell body than distal axotomy sites in *zdIs5*.

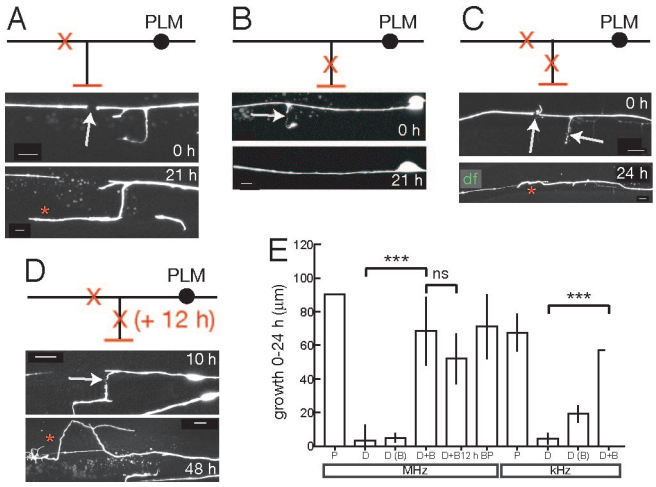

Fig. 4. The touch neuron synaptic branch inhibits regrowth of the distal axon. All animals were cut in mid L4 stage, *zdIs5* marker. (*A*) The PLM distal process does not regrow after cutting; in some animals, the synaptic branch grows in response (*). (*B*) Retraction of PLM synaptic branch stump after cutting (arrow). (*C*) The distal process regrows when the branch is also cut. (*D*) Distal axon regrowth stimulated when the branch is cut 12 h after the distal axon. Anterior is to the left and dorsal up in all panels. (Scale bars: *A–C*, 5 μm; *D*, 10 μm.) (*E*) Process regrowth in 24 h after kHz or MHz axotomy of proximal (P), distal (D) axon, or distal + branch (D+B), or branch point (BP); also plotted is branch growth after cutting distal axon [D(B)]; $n = 6–15$ for each group; comparisons use t test. ***, $P < 0.001$; ns, not significant. Axon growth after the delayed branch cut (*D*) is measured between 24 and 48 h after the first cut.

PLM axons regrew less when cut far from the cell body compared with cutting closer; we found a similar effect of absolute distance in ALM (SI Fig. 8*E*). Thus, although axons cut further from the cell body regrow less, this effect is independent of the influence of the synaptic branch point.

The synaptic branch of ALM/PLM marks a transition between the proximal axon, which can regrow after injury, and the distal axon, which cannot. Because cutting the branch itself caused it to retract and disappear, we tested whether cutting both the distal axon and the branch could reverse the inability of the distal axon to regrow. Strikingly, when the branch was also cut, the distal axon of PLM regrew to an extent similar to that seen after cutting the proximal axon (Fig. 4 *C* and *E*). Ablation of the branch point itself also resulted in regrowth from the proximal stump (BP, Fig. 4*E*). These findings suggest that axotomy results in an intrinsic change to the cell. To test whether such a change persists in time we cut the PLM branch 10–12 h after cutting the distal axon, and found that this also strongly stimulated distal regeneration, equivalent to that after simultaneous cutting (Fig. 4 *D* and *E*). We infer that cutting the distal axon results in a long-lasting change to the cell, and that regrowth from the distal stump is actively blocked by the presence of the synaptic branch.

Discussion

We show that multiple *C. elegans* neuron types can regenerate after laser induced damage. Motor and sensory neurons also undergo regenerative growth in *C. elegans* β-spectrin mutants, in which axons undergo cycles of breakage and regeneration because of axon fragility (28). Regeneration of injured neurons is common in other invertebrates (29), and our findings reinforce the view that *C. elegans* neurons have a high capacity for regrowth after injury. As in other animals, the propensity of a *C. elegans* neuron to regenerate is affected by a complex set of environmental and intrinsic factors.

Axons cut using laser axotomy undergo a stereotyped sequence of events. At the time of cutting a break of less than a

NEUROSCIENCE

micrometer in length is made; these breaks expand over the course of the next few hours. These short-range retractions appear distinct from the acute degeneration of axons observed by using live imaging in mice, where cut ends die back hundreds of microns within 30 min of injury (30). Fusion of the cut ends was more often seen after the more precise cutting by using amplified lasers (21), but less so after MHz axotomy, which creates an area of damage that likely physically blocks the regrowing process. Nevertheless in several animals we observed the regrowing process grow around the damaged area and fuse with the distal fragment, suggesting regrowing axons can recognize their distal fragments and will tend to fuse with them if they form contacts.

After axotomy an axon typically displays a quiescent period of between 6 and 24 h, after which a new growth cone can be seen at the proximal stump. Motility of the regenerated growth cones was highest over the next 36 h and then declined. In our experiments axons regrew at up to 10 μm/h; if regrowing growth cones move discontinuously then their actual maximum rate may be higher. As VD growth cones can travel up to 60 μm/h in intact animals (31) these results suggest that regenerating *C. elegans* axons grow more slowly than in normal development.

Developmental Changes in Regrowth. We found two main differences in the regrowth of early larval versus late larval or young adult axons. The amount of regrowth of touch neurons declined slightly from L1 to L4 stages; this seemed to reflect a longer quiescent period before regrowth commenced, as L4 stage axons eventually could regrow at the same rate as L1 axons. Only in young adults did the maximum rate of extension decline. Developmental changes in axon extension rates have been observed in several organisms (32–34) and may contribute to declines in ability to regenerate. Our findings suggest that such developmental declines can be analyzed even in the rapidly developing *C. elegans* nervous system.

Second, guidance errors in regrowth increased with age. Several factors could account for the decrease in accuracy. Regrowing axons have further to go in later stages, and thus have more potential room for error. If guidance cues for the touch neurons are distributed in gradients these may be less effective if spread out over the larger scale of the L4 animal. Touch neurons also undergo ensheathing by surrounding epidermal cells that could block extracellular signals, leading to inaccurate regrowth (35). Finally, aberrant sensitivity to cues such as the ephrins may contribute to guidance errors. Dorsal growth of D commissures in embryos and L1 animals depends on repulsion from a ventral source of UNC-6/netrin (36). As UNC-6 also directs later dorsal guidance events such as the migration of gonadal distal tip cells in the L3 stage (37), it is likely that enough UNC-6 gradient remains in the L4 stage to accurately guide D neurons.

Eph Signaling and Regeneration. In wild type late larvae and adults, regenerating touch neuron axons deviated far from their original trajectory and often reversed direction. *vab-1* mutant axons deviated significantly less and showed significantly fewer reversals. Misguidance of regenerating PLMs in the wild type could reflect increased sensitivity of the regenerating axons to repellent cues in the anterior, consistent with a repulsive role for Eph signaling in PLM termination. As regenerating PLMs typically reverse before their normal termination point, such repellent cues may be broadly distributed. We speculate that anteriorly localized ephrins regulate both the direction of growth and the termination position of the PLM neurons. *C. elegans* ephrins are widely distributed in neuronal and epidermal cells (38, 39), and further work will be required to determine their cellular focus in touch neuron regrowth. Ephrin signaling both promotes and inhibits regeneration in vertebrates. Regeneration of a topographic retinotectal map in amphibians is likely dependent on expression of ephrins and their receptors (40), and up-regulation of EphB3 after injury contributes to the regrowth of retinal ganglion cells (41). By contrast, ephrin-B3 is an inhibitory component of CNS myelin (24), and elimination of its receptor EphA4 enhances regeneration of the corticospinal tract (42).

Role of Branches. We find a sharp transition in regenerative ability at the touch neuron synaptic branch, independent of distance from the cell body. What is it about the synaptic branch that exerts such a strong effect on regrowth? Because cutting the branch at any position causes the stump to disappear, it is unclear whether the branch junction, the branch itself, or synapses made by the branch, account for this effect. In animals lacking the RPM-1 ubiquitin ligase, PLM synaptic branches extend normally but later retract; concomitantly the axon itself grows into the ventral nerve cord (27). The *rpm-1* phenotype suggests the PLM branch or its synapses inhibit axon growth. However, axotomy of the branch alone does not stimulate growth of the distal axon. Retraction of the branch stump may eliminate a "damage" signal that would otherwise lead to regrowth. Alternatively, inhibition of axon growth by synaptic signaling may only be effective in a critical period of synaptogenesis.

We speculate that a sorting area at the PLM branch point routes presynaptic components to the branch and not further along the axon. After the distal axon is severed, growth is stimulated, presumably requiring increased delivery of membrane from the soma. When the branch is present such components are mostly sorted to the branch. In contrast, when the branch is absent the sorting area disappears and the distal axon is now able to grow at the site of axotomy. Branch points of dendritic arbors contain Golgi outposts that may play a role in dendrite growth (43, 44). A Golgi outpost like structure at the PLM branch point could participate in sorting to the presynaptic branch. If this structure requires the synaptic branch itself for stabilization, loss of the branch by axotomy or lack of RPM-1 may lead to loss of sorting and of the distinction between distal and proximal in the axon. Tests of this model will require identification of molecules acting at the branch point itself. The effects of cutting the branch may also be analogous to "conditioning lesion" paradigms (12), in which axotomy of a peripheral branch stimulates regrowth of a central axon. Further analysis should reveal whether additional similarities exist at the level of molecular mechanism.

Materials and Methods

Genetics. *C. elegans* strains were maintained on nematode growth medium (NGM) agar plates using standard procedures at 20°C–23°C. We used the following mutations: *vab-1*(*e2027*, *dx14*, *e118*) (45), *efn-1*(*ju1*) (39). To visualize D type motor neurons, we used P*unc-25*-GFP *juIs76* (46); to mark DDs, we used P*flp-13*-GFP transgenes *juIs145* (J. Meir and Y.J., unpublished results) or *ynIs37* (47). We used two transgenes to mark the touch neurons: *zdIs5* (P*mec-4*-GFP) and *muIs32* (P*mec-7*-GFP). *zdIs5* drives GFP expression in the six touch neurons (48); *muIs32* is also weakly expressed in several other cell types. To mark phasmids PHA and PHB, we used P*srb-6*-GFP *gmIs12* (49) and to mark the AWB neurons we used P*str-1*-GFP *kyIs104* (50).

Femtosecond Lasers. In most experiments described here, we used a KMLabs MTS Ti-Sapphire oscillator (Kapteyn-Murnane Laboratories, Boulder, CO) pumped by a Verdi V5 (Coherent, Santa Clara, CA). The measured pulse energy of this oscillator was 3.4 nJ at a repetition rate of 94 MHz and wavelength of 790–800 nm. We used a home-built autocorrelator to measure a pulse duration of 150 fs (FWHM). In more recent experiments, we used a KMLabs Cascade laser that can be operated in mode-locked continuous wave (80 MHz) or cavity-dumped (1–100 kHz)

modes (SI Table 1). In some configurations, we used a spatial filter to clean and expand the beam. We attenuated the pulse energy using neutral density filters and controlled pulse delivery with an electro-mechanical shutter (Uniblitz VS14 with VMM-T1 controller; Vincent Associates, Rochester, NY). The laser beam enters the side port of a Zeiss Axiovert 200 (Carl Zeiss, Jena, Germany) equipped with a dual camera attachment and reflects off a mirror and through a Planapo ×100x/N.A. 1.4 objective to the specimen. GFP-labeled axons were visualized by using epifluorescence and a Hamamatsu Orca camera (Hamamatsu Photonics, Hamamatsu City, Japan) controlled by Improvision Volocity software (Improvision, Lexington, MA). Custom filters (Chroma Technology, Rockingham, VT) were used to ensure transmission of the laser beam. To anesthetize animals for surgery and imaging, we used 0.1–1% 1-phenoxy-2-propanol (TCI America, Portland, OR) in M9 buffer and in the agar pad.

After axotomy, we occasionally observed faint GFP expression in nearby cell bodies and processes, beginning several hours after cutting. Such ectopic expression may be due to laser-induced membrane fusion and GFP mixing between the axotomized cells and adjacent processes. Membrane fusion induced by UV laser irradiation has been observed in *C. elegans* embryos and oocytes (51, 52). We scored regrowth of a cut axon in such cases only when it could be unambiguously distinguished from ectopic GFP expression in a neighboring process.

Conventional Laser. We also used a Photonics Micropoint VSL pulsed UV laser (Photonics Instruments, St. Charles, IL). The laser beam is delivered to a Zeiss Axioplan 2 Imaging microscope equipped for simultaneous laser and GFP illumination via a Photonics Instruments adaptor, and surgery was performed by using a Plan Neofluar ×100/N.A. 1.3 objective.

Confocal Imaging. We used a Zeiss Pascal or LSM510 confocal to acquire z stack images of live anesthetized worms. Images are projections or single slices of confocal *z* stacks made from slices 0.3–1 μm apart. Process lengths are calculated from maximum transparency projections of a single *z* stack, by using the Zeiss AIM software. Because axons also grow in the *z* axis (i.e., the left-right axis of the animal), these measurements systematically underestimate total process lengths. All statistical analyses used GraphPad Prism (GraphPad Software, San Diego, CA).

We thank Scott Clark for insightful comments on the manuscript and members of the A.D.C. and Y.J. laboratories for discussions. We thank Aravinthan Samuel for advice, and members of the J.Z.Z. laboratory especially Adam Schwartzberg, Leo Seballos, and Abe Wolcott, for their help with the laser at the University of California, Santa Cruz. J.Z.Z. is grateful for financial support from the National Science Foundation, the Department of Energy, and the University of California, Santa Cruz. Y.J. is an Investigator of the Howard Hughes Medical Institute. Work in A.D.C.'s laboratory is supported by National Institutes of Health Grant R01 GM54657.

1. Ramon y Cajal S (1913–14) *Estudios sobre la degeneración y regeneración del sistema nervioso* (Moya, Madrid).
2. Gitler D, Spira ME (1998) *Neuron* 20:1123–1135.
3. Chierzi S, Ratto GM, Verma P, Fawcett JW (2005) *Eur J Neurosci* 21:2051–2062.
4. Verma P, Chierzi S, Codd AM, Campbell DS, Meyer RL, Holt CE, Fawcett JW (2005) *J Neurosci* 25:331–342.
5. Liu RY, Snider WD (2001) *J Neurosci* 21:RC164.
6. Benfey M, Aguayo AJ (1982) *Nature* 296:150–152.
7. Schwab ME (2004) *Curr Opin Neurobiol* 14:118–124.
8. Silver J, Miller JH (2004) *Nat Rev Neurosci* 5:146–156.
9. Fournier AE, GrandPre T, Strittmatter SM (2001) *Nature* 409:341–346.
10. Park JB, Yiu G, Kaneko S, Wang J, Chang J, He XL, Garcia KC, He Z (2005) *Neuron* 45:345–351.
11. Alabed YZ, Grados-Munro E, Ferraro GB, Hsieh SH, Fournier AE (2006) *J Neurochem* 96:1616–1625.
12. Neumann S, Woolf CJ (1999) *Neuron* 23:83–91.
13. Becker T, Wullimann MF, Becker CG, Bernhardt RR, Schachner M (1997) *J Comp Neurol* 377:577–595.
14. Bhatt DH, Otto SJ, Depoister B, Fetcho JR (2004) *Science* 305:254–258.
15. Leyssen M, Ayaz D, Hebert SS, Reeve S, De Strooper B, Hassan BA (2005) *EMBO J* 24:2944–2955.
16. MacDonald JM, Beach MG, Porpiglia E, Sheehan AE, Watts RJ, Freeman MR (2006) *Neuron* 50:869–881.
17. Yanik MF, Cinar H, Cinar HN, Chisholm AD, Jin Y, Ben-Yakar A (2004) *Nature* 432:822.
18. Chung SH, Clark DA, Gabel CV, Mazur E, Samuel AD (2006) *BMC Neurosci* 7:30.
19. Bargmann CI, Avery L (1995) *Methods Cell Biol* 48:225–250.
20. Newman AP, White JG, Sternberg PW (1996) *Development (Cambridge, UK)* 122:3617–3626.
21. Yanik MF, Cinar H, Cinar N, Gibby A, Chisholm AD, Jin Y, Ben-Yakar A (2006) *IEEE J Sel Top Quantum Electron* 12:1283–1291.
22. Gallegos ME, Bargmann CI (2004) *Neuron* 44:239–249.
23. Kullander K, Klein R (2002) *Nat Rev Mol Cell Biol* 3:475–486.
24. Benson MD, Romero MI, Lush ME, Lu QR, Henkemeyer M, Parada LF (2005) *Proc Natl Acad Sci USA* 102:10694–10699.
25. Mohamed AM, Chin-Sang ID (2006) *Dev Biol* 290:164–176.
26. Egea J, Klein R (2007) *Trends Cell Biol* 17:230–238.
27. Schaefer AM, Hadwiger GD, Nonet ML (2000) *Neuron* 26:345–356.
28. Hammarlund M, Jorgensen EM, Bastiani MJ (2007) *J Cell Biol* 176:269–275.
29. Anderson H, Edwards JS, Palka J (1980) *Annu Rev Neurosci* 3:97–139.
30. Kerschensteiner M, Schwab ME, Lichtman JW, Misgeld T (2005) *Nat Med* 11:572–577.
31. Knobel KM, Jorgensen EM, Bastiani MJ (1999) *Development (Cambridge, UK)* 126:4489–4498.
32. Bray D, Bunge MB, Chapman K (1987) *Exp Cell Res* 168:127–137.
33. Blackmore M, Letourneau PC (2006) *J Neurobiol* 66:348–360.
34. Jones SL, Selzer ME, Gallo G (2006) *J Neurobiol* 66:1630–1645.
35. Emtage L, Gu G, Hartwieg E, Chalfie M (2004) *Neuron* 44:795–807.
36. Wadsworth WG, Bhatt H, Hedgecock EM (1996) *Neuron* 16:35–46.
37. Su M, Merz DC, Killeen MT, Zhou Y, Zheng H, Kramer JM, Hedgecock EM, Culotti JG (2000) *Development (Cambridge, UK)* 127:585–594.
38. Wang X, Roy PJ, Holland SJ, Zhang LW, Culotti JG, Pawson T (1999) *Mol Cell* 4:903–913.
39. Chin-Sang ID, George SE, Ding M, Moseley SL, Lynch AS, Chisholm AD (1999) *Cell* 99:781–790.
40. Bach H, Feldheim DA, Flanagan JG, Scalia F (2003) *J Comp Neurol* 467:549–565.
41. Liu X, Hawkes E, Ishimaru T, Tran T, Sretavan DW (2006) *J Neurosci* 26:3087–3101.
42. Goldshmit Y, Galea MP, Wise G, Bartlett PF, Turnley AM (2004) *J Neurosci* 24:10064–10073.
43. Horton AC, Ehlers MD (2003) *J Neurosci* 23:6188–6199.
44. Ye B, Zhang YW, Jan LY, Jan YN (2006) *J Neurosci* 26:1063110632.
45. George SE, Simokat K, Hardin J, Chisholm AD (1998) *Cell* 92:633–643.
46. Huang X, Cheng HJ, Tessier-Lavigne M, Jin Y (2002) *Neuron* 34:563–576.
47. Kim K, Li C (2004) *J Comp Neurol* 475:540–550.
48. Clark SG, Chiu C (2003) *Development (Cambridge, UK)* 130:3781–3794.
49. Hawkins NC, Ellis GC, Bowerman B, Garriga G (2005) *Dev Biol* 284:246–259.
50. Troemel ER, Chou JH, Dwyer ND, Colbert HA, Bargmann CI (1995) *Cell* 83:207–218.
51. Schierenberg E (1984) *Dev Biol* 101:240–245.
52. Irle T, Schierenberg E (2002) *Dev Genes Evol* 212:257–266.